EFFECT OF GE ON OXIDATION BEHAVIOR OF 60% CU – 40% ZN MUNTZ METAL

Ekbal Mohammed Salih [1]– Hayder J. Karim [1] – Kadhim F. Al-Sultani[1] – Zainab Al-Khafaji[2, 3*]

[1] Materials Engineering College, University of Babylon, Iraq.
[2] Building and Construction Engineering Technology Department, Al-Mustaqbal University College, Babylon, Iraq
[3] Department of Civil Engineering, Faculty of Engineering and Built Environment, Universiti Kebangsaan Malaysia, 43600 UKM Bangi, Selangor, Malaysia.

ARTICLE INFO

***Article history*:**
Received: 11.04.2023.
Received in revised form: 04.05.2023.
Accepted: 29.01.2024.

Keywords:
Brass
Muntz metal Cu–Zn alloy
alloying elements
Germanium
heat exchangers
dezincification

DOI: https://doi.org/10.30765/er.2201

Abstract:

Copper–base alloys are widely used in Marine industries and heat exchangers. Muntz Metal 60% Cu – 40% Zn is one of the critical Cu alloys used in decoration, tubing for heat exchangers, and Marine environments, but it is subject to dezincification and stress–correction cracking. This study employed alloying elements (Al, Sn, Ge) to achieve their properties (oxidation behavior, thermal shock resistance, mechanical and corrosion resistance). All results confirmed that an enhancement in properties, Ge, plays an essential role in this enhancement due to the formation of protective non-pours oxide layers from GeO2 and AL2O3 layers. Also, adding (Sn) made the alloy's microstructure very fine. These elements improve hardness and reduce corrosion rate by 83%, while in the oxidation test, the reduction in specific weight change was equal to 99%. Also, a significant improvement in thermal shock resistance concerning the reference sample was achieved.

1 Introduction

Oxidation is a kind of metallic corrosion that takes place once oxygen forms on the surface of the metal throughout an ionic chemical reaction [1]–[5]. Electrons undergo a transfer from metallic substances to the oxygen molecules in this process. Subsequently, negative oxygen ions are generated inside the metal, resulting in the formation of an oxide-laden surface. In the case of copper, oxidation happens when copper is exposed to air, but corrosion may also be induced by salt water, acidic chemicals, and heat [6]–[9]. It is well known that copper is one of the essential materials due to its good electrical, thermal, and mechanical properties used in electrical cables, wires, and heat exchangers [10]; two main types of alloys have copper: brass which zinc is the second element as well as copper its concentration starts from low to 40% Zn, the second alloy is bronze, other elements (AL, Sn, Ni) are added to copper to improve metallurgical and properties [11]–[14]. (α and β) The most common phases in brasses depend on the % of Zn, usually up to 37% Zn. It is a single phase (α) that is characterized by soft (cold work); if Zn increases, other phases will appear (β): hard (hot work).

The quantity of (β) phase increases as % of Zn increases or other alloying elements are added (zinc equivalence) [8], [15]–[17]. Muntz metal (60% Cu, 40% Zn), whose commercial composition is Muntz metal C 28000 [18], 60% Cu– 40% Zn, is a critical alloy due to its high strength; this alloy is excellent hot for mobility, but have low ductility, at Room temperatures and use in many applications: architectural panel, sheets, nuts, bolts, condenser platter, brazing rot and heat exchanger, condenser tubing, hot forging this alloy and other types of alloys [19], suffer from common deterioration (dezincification or selective leaching) especially when exposing to the electrolyte (sea water), which mean corrosive attack of a particular element (Zn usually) rather than copper. Also, this alloy suffers from oxidation, thermal shock in high temperatures, and low ductility; these problems limit the use of this alloy in marine or thermal media. Several studies have been carried out to enhance and improve mechanical, electrical, and oxidation properties by adding several

* Corresponding author
E-mail address: p123005@siswa.ukm.edu.my

elements (Al, Sn, Ge) [20]–[22]. In this study, alloying element (Ge) has been added, as well as Al, Sn, to the alloy Muntz Metal to improve it is oxidation resistance and thermal shock (heating at high temperature then cooling suddenly in the air) as well as mechanical and corrosion resistance.

2 Experimental work

2.1 Prepare alloys by casting.

The melting and casting process has been used to prepare base alloy and others after adding alloying elements (AL, Sn, Ge). Table (1) represents the chemical composition of all specimens of alloy used in this study.

Table 1. Chemical composition of alloys.

Alloys	Cu%	AI%	Sn%	Ge%	Pb%	Zn%
Base alloy	Bal.	-	-	-	1.5	38.38
B1	Bal.	2.2	0	0	1.4	39.18
B2	Bal.	2.4	2.5	0	1.4	39.18

The melting temperature of copper (Cu) is 1083°C, zinc (Zn) is 419.6°C, aluminum (Al) is 660^{o}C, tin (Sn) is 231.9^{o}C, germanium (Ge) is 938.2^{o}C, and lead (Pb) is 327.5^{o}C, while the melting temperature of the base alloy is 906°C so that Zinc element has been added as % compensatory to compensate the missing of (Zn) during the melting process before casting. All melted elements are mixed alloy and then poured into a cylinder metallic mold with a dimension of 20 mm diam., 130mm high; before casting, the die was heated with graphite lubricant, the molten alloy was poured into the mold and left to solidify to room temperature.

2.2 Specimen Preparation

After solidification, all alloys were cut by turning machine (B, B1, B2, B3) into a disc shaping with dimension (20 X5) mm as shown in Figure (1).

Figure 1. Specimens (B, B1, B2, B3).

According to standard metallographic techniques, all specimens were prepared, which included grinding (several steps) and then polishing by using a diamond with particle size (1ṅm), washing with distilled water, then drying and etching using the solution of (5 grams of $FeCl_3$ + 2 cm³ Hcl + 95 cm³ methylated spirit) for the period (10-15) sec washed and dry after these processes, all samples are ready for microstructure test.

3 Tests

3.1 XRD

X-ray measurement conditions were Target Cu, λcu = 1.5 40 60 A°, current and voltage was 15m A and 30Kv, respectively, range and speed scanning was 20 = (0 to 100) degree and 2 deg. / min respectively Figure (2, 3, 4, 5) represented x-ray patterns of all specimens (Base, B1, B2, B3), respectively.

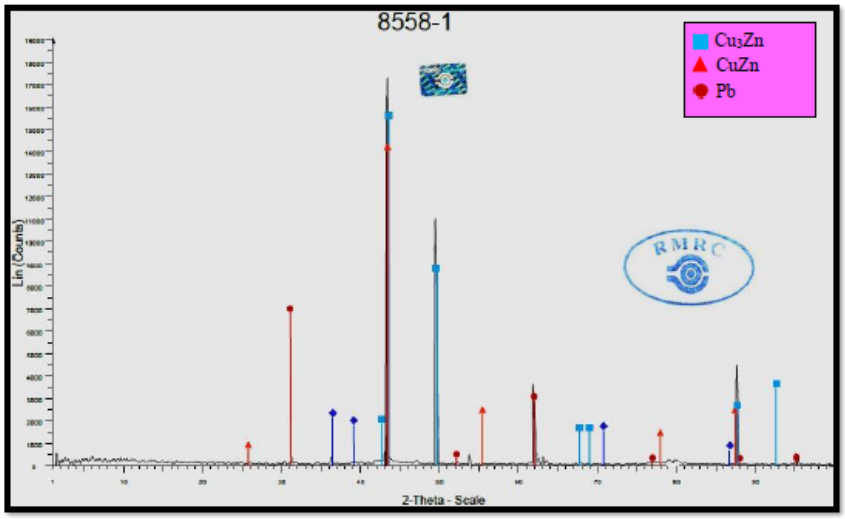

Figure 2. X-Ray Diffraction Analysis for B, Base Alloy.

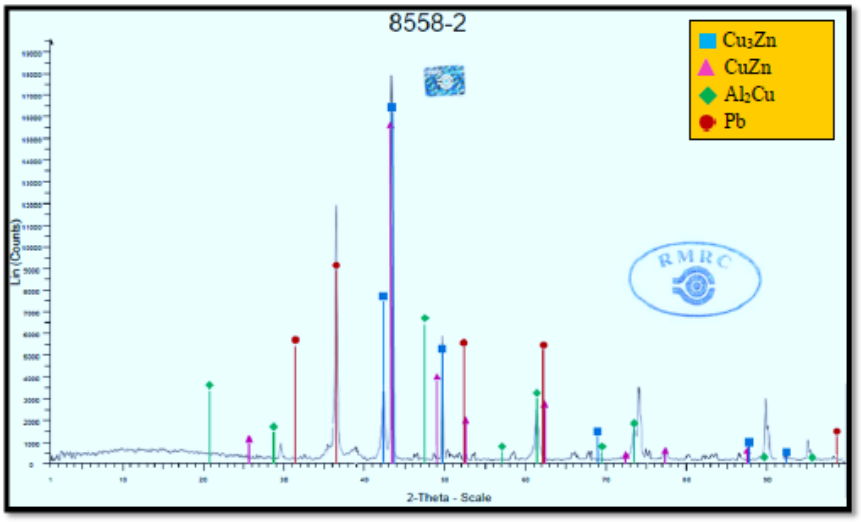

Figure 3. X-Ray Diffraction Analysis for B1 (Cu, Zn, Al).

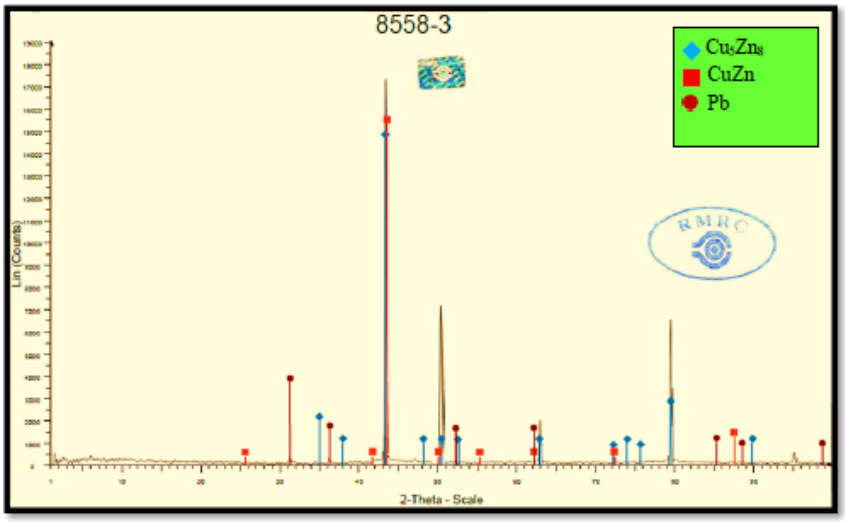

Figure 4. X-Ray Diffraction Analysis for B2 (Cu, Zn, Al, Sn).

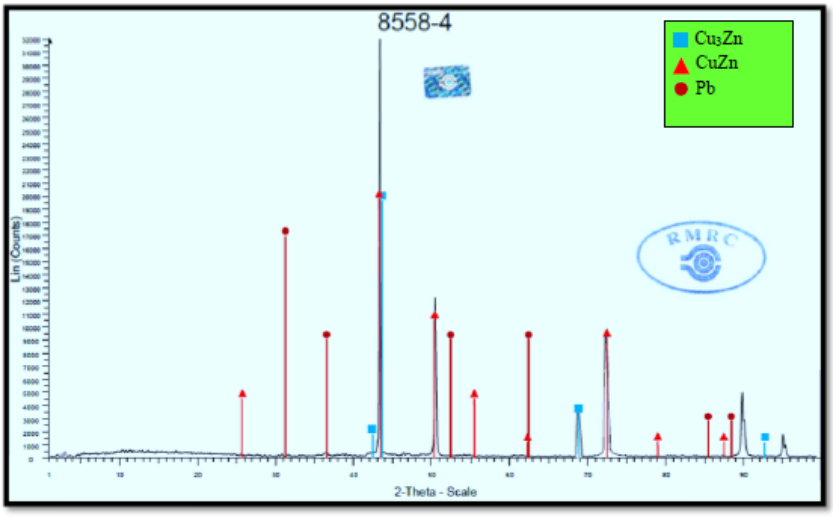

Figure 5. X-Ray Diffraction Analysis for B3 (Cu, Zn, Al, Ge).

3.2 Microstructure

LOM has been used to examine the microstructures of all specimens, Figure (6, 7, 8, 9) shows microstructures of all samples.

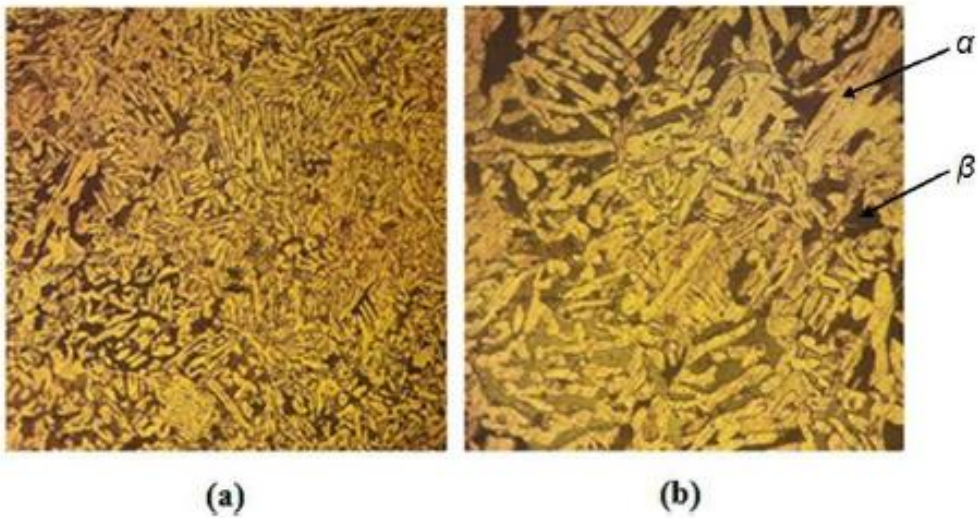

Figure 6. Light Optical Microstructure for B, Base Alloy. a (100x), b (200x).

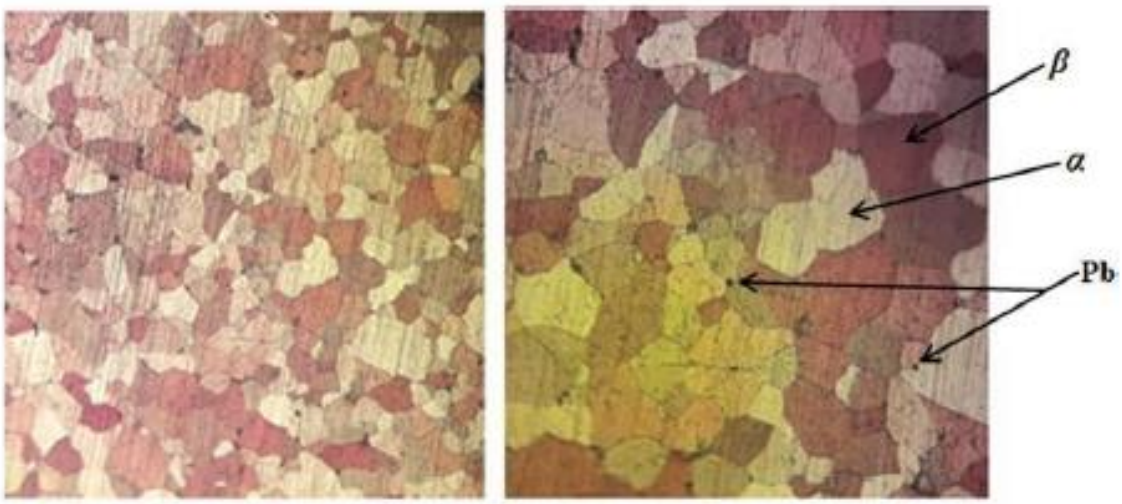

Figure 7. Light Optical Microstructure for B1 a (100x), b (200x).

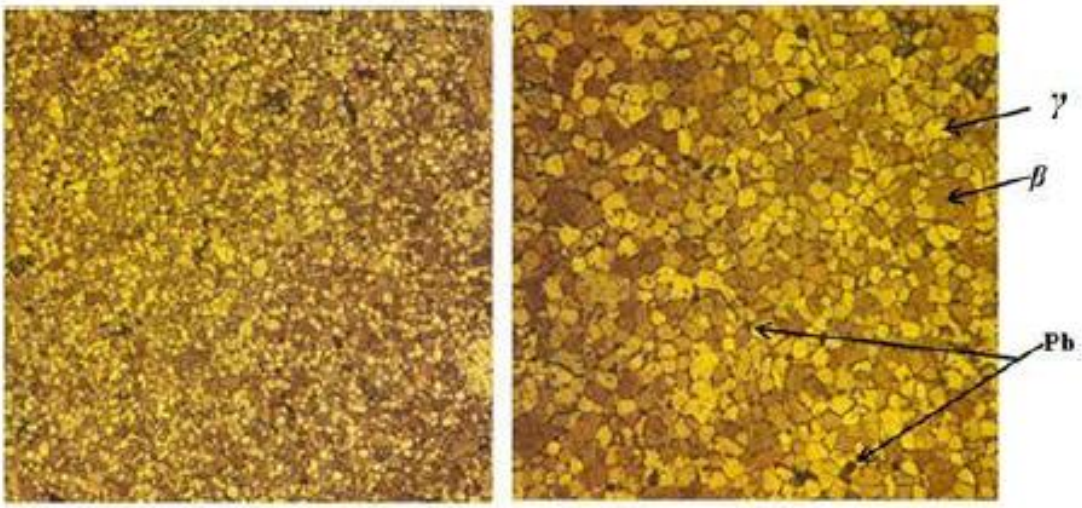

Figure 8. Light Optical Microstructure for B2 a (100x), b (200x).

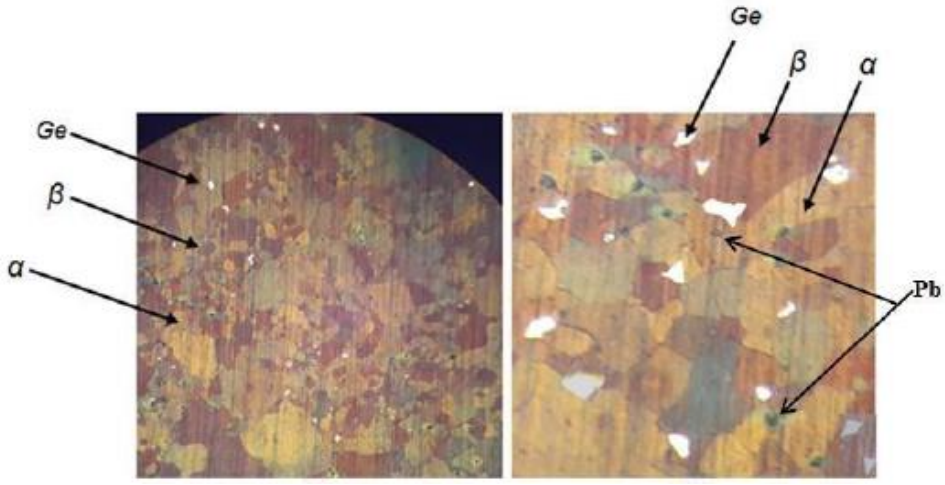

Figure 9. Light Optical Microstructure for B3 a (100x), b (200x).

3.3 SEM + EDS

SEM has been taken using the TESC AN S8000 model, USA, according to ASTMG54 [23]. Figure (10, 11, 12) The cross-sectional SEM image shows oxide layers for base metal and B3 (after oxidation in the air) in cyclic oxidized at 600ºC and 700ºC for 60 hrs., each cycle 5 hrs.

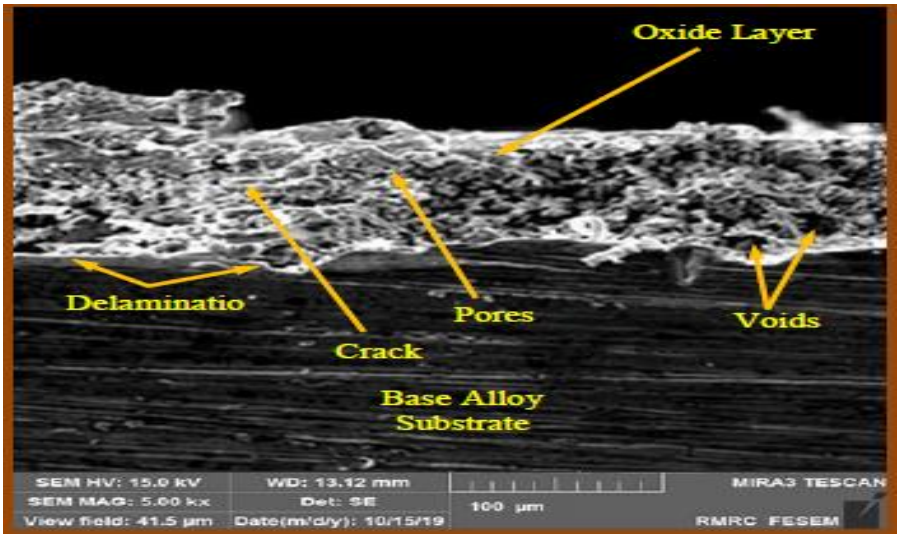

Figure 10. Cross-Sectional SEM Image Showing Defects (cracks, voids, pores) for Specimen B.

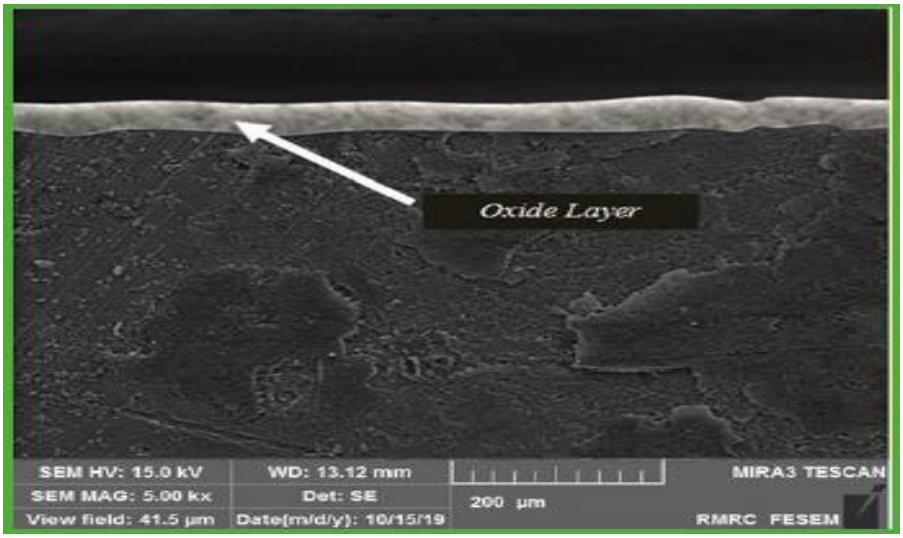

Figure 11. Cross-Sectional SEM Image for Alloy B3 at 600 ºC.

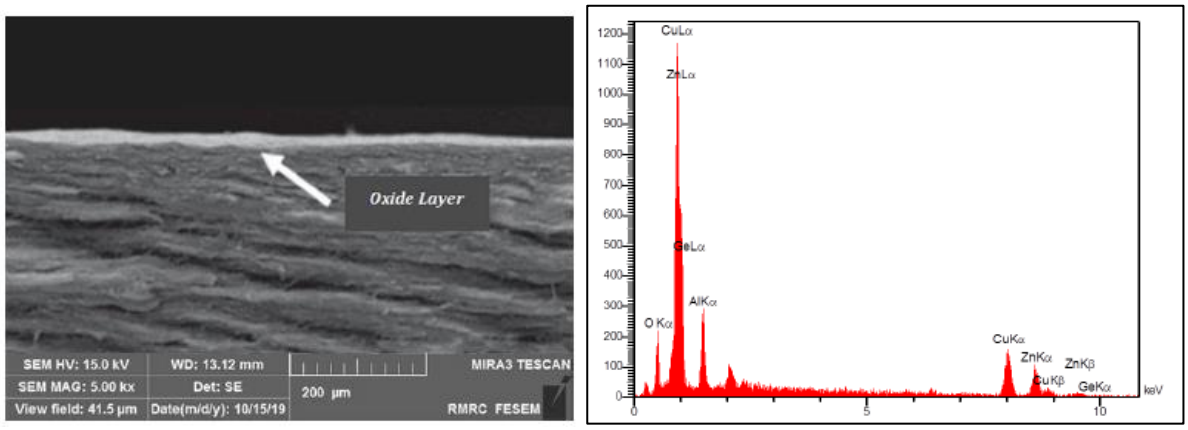

a *b*

Figure 12. a) Cross-Sectional SEM Image for Alloy B3 at 700 °C, b) EDS Analysis for Surface Morphology of Specimen B3.

3.4 Vicker hardness

According to ASTM E99-17, a microhardness test was carried out by using a hardness tester (HVS – 1000) digital at loading (500g) for a (15) second hold. Table (2) shows hardness and improvement for all samples.

Table 2. The hardness of all Examined Specimens.

Alloy Specimens	Vickers hardness (HV) g/mm^2	Improvement %
B, Base Alloy, (α, β)	110	-
B1, (Base Alloy+ A1)	141	28.5
B2, (Base Alloy+ A1 +Sn)	183	66.5
B3, (Base Alloy+ A1 +Ge)	136	24

3.5 Corrosion Test

According to ASTM G31-72, all specimens were wholly immersed in a salt solution (3.5% NaCl). All samples were taken out to examine the loss in mass after every (3 days) of immersion at room temperature. The period of immersion was (133days). The relationship calculated corrosion rate:

$$\text{C.R}\ \frac{g}{cm^2.day} = \frac{change\ in\ weight\ (g)}{sur\ face\ Area\ A^2.immersion\ time\ day}$$

Figure (13) represents Base alloy suffering de – alloying (dezincification) after (133 days) of immersion in 3.5% NaCl. Figure (14) shows the fitting curve of the simple immersion test for all samples in salt solution after (170 days).

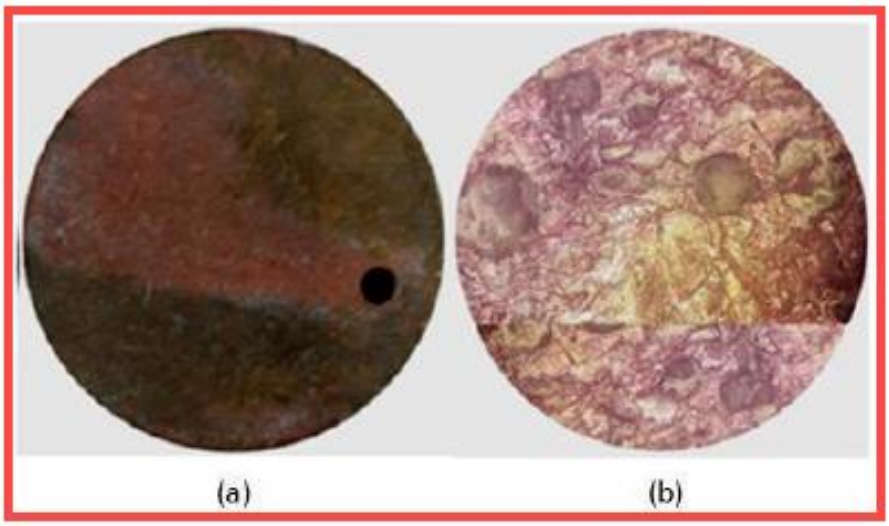

Figure 13. a) base alloy suffers from d-alloying, selective leaching during immersion in a salt solution, b) microstructure under light optical microscopy (400x).

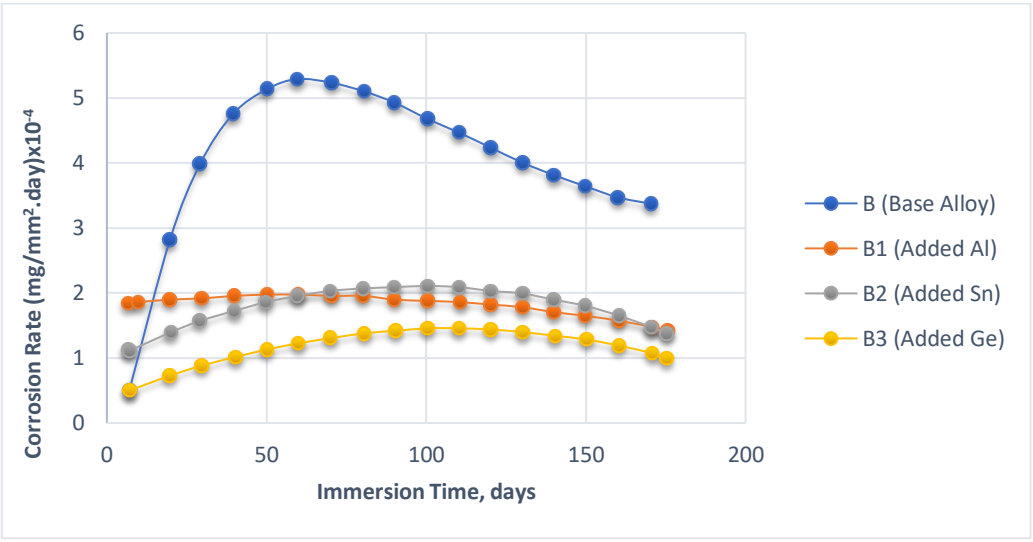

Figure 14. Fitting Curves of Simple Immersion Test for All Specimens in Salt Solution for immersion Period (170 days).

3.6 Oxidation Test

3.6.1. Cyclic Oxidation

Oxidation is a common type of degradation when the material is exposed to high-temperature environments. All specimens were conducted at temperatures (500, 600, 700, and 750) ^{o}C in the air; the oxidation behavior of each sample was evaluated by heating the alloy in the furnace at test temperature and weighting them every 5 hrs. by removing the specimen from the furnace after allowed them to cool (in the furnace), cleaned to detach the spalled oxide and weight change per unit surface area has been calculated. Table (3) represents an improvement in specific weight at different temperatures and improvement according to the reference sample.

Table 3. Improving in Specific Weight Change at Steady State.

Alloy	Weight change at 500 °C (mg/cm2)	Improving %	Weight change at 500°C (mg/cm2)	Improving %	Weight change at 500 °C (mg/cm2)	Improving %	Weight change at 500°C (mg/cm2)	Improving %
B	4.4	-	29	-	53	-	68	-
B 1	0.072	98.4	0.205	99.3	0.84	98.4	1.02	98.5
B 2	0.124	97.2	0.245	99.2	1	98.1	1.13	98.3
B 3	0.044	99	0.120	99.6	0.58	99	0.78	98.9

While Figure (15,16) shows a relative weight change at different temperatures concerning base alloys and alloys (B1, B2, B3).

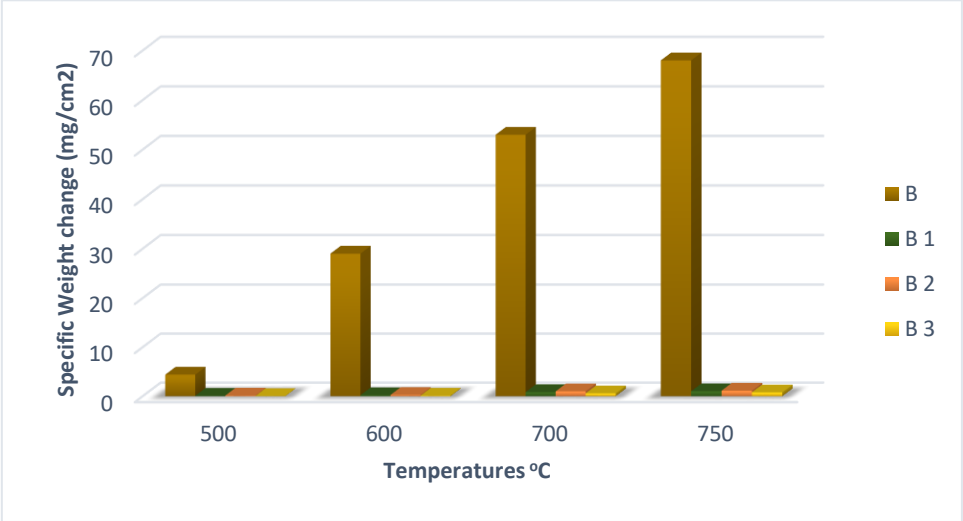

Figure 15. Comparative in weight change at different temperatures concerning base alloy (B).

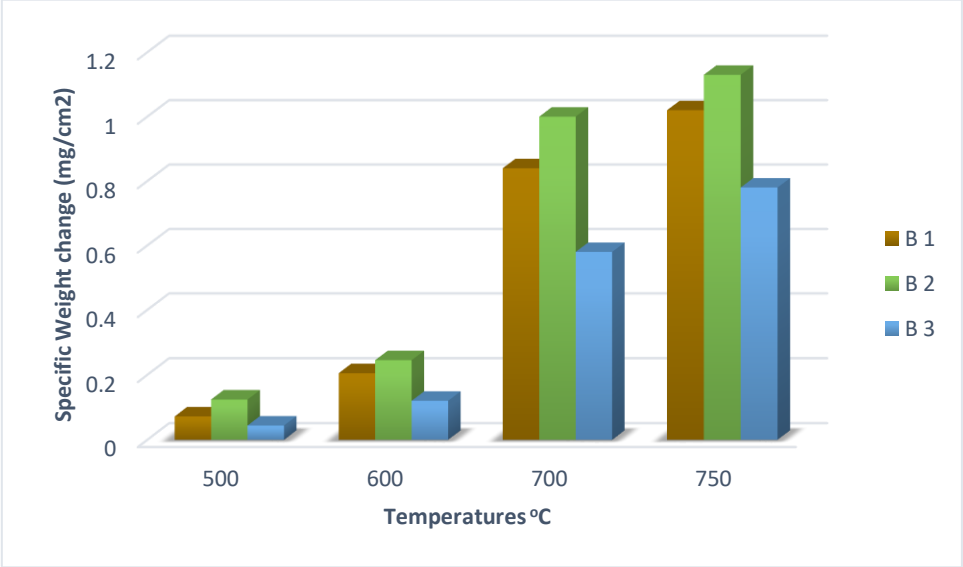

Figure 16. Comparative weight change at different alloy temperatures (B1, B2, B3).

3.6.2. Thermal Shock

Thermal Shock is a term used to describe the thermal stresses the body is exposed to due to sudden temperature changes. All alloys were tested at different temperatures after (60 hrs.) oxidation time, then suddenly taken out of the furnace and cooled to room temperature (cool in the air); their weight was measured, then returned to the furnace again, and so on. Figure (17) shows the thermal shock effect of all samples after sudden cooling in the air for (60hrs.) at 650°C and 750°C, While Figure (18,19) show the effect of thermal stress on the oxide surface structure of all samples (B1, B2, B3) after sudden cooling in the air at 650-750°C.

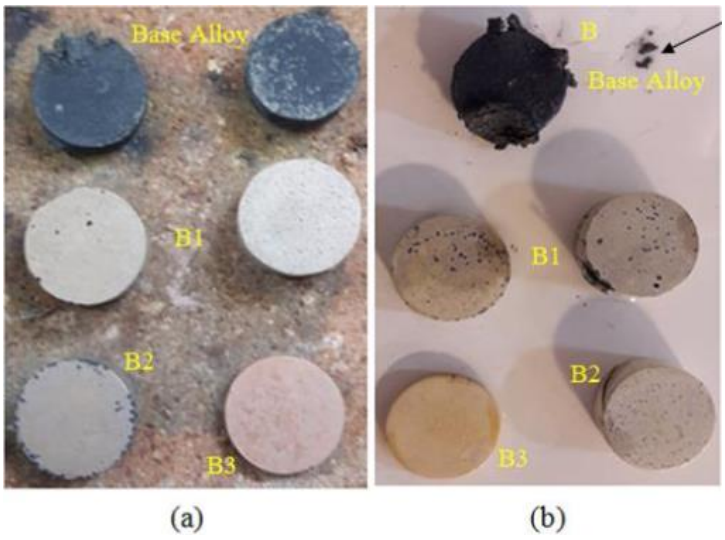

Figure 17. Effect of Thermal Shock of specimen alloys after sudden cooling in the air for 60 hrs: a) at 650 °C, b) at 750 °C.

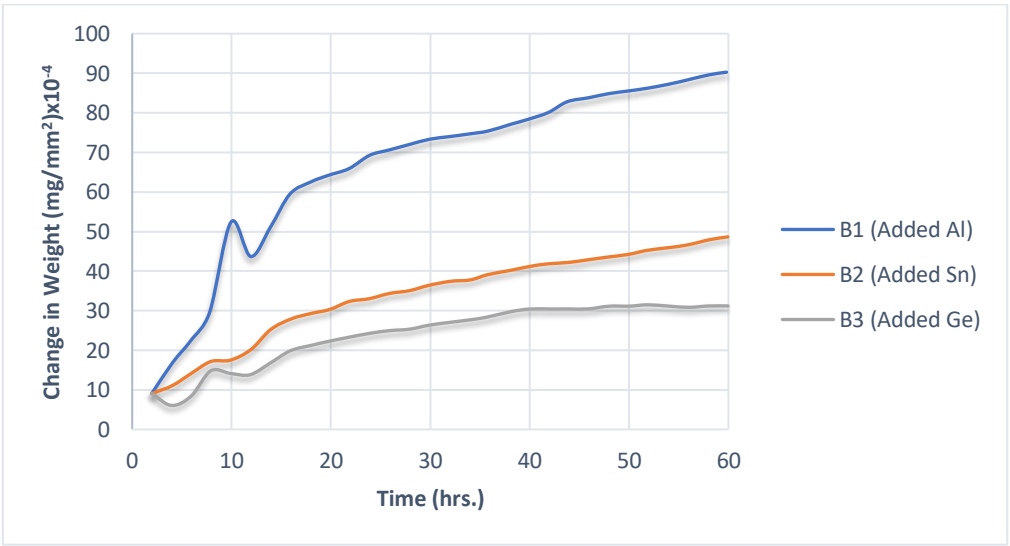

Figure 18. Effect of Thermal Shock on Oxide Surface Structure of Alloys (B1, B2, and B3) after Sudden Cooling in Air at 650°C.

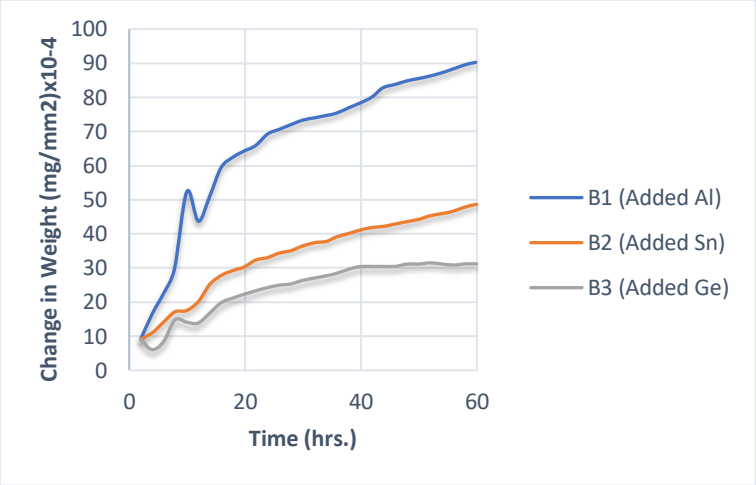

Figure 19. Effect of Thermal Shock on Oxide Surface Structure of Alloys (B1, B2, and B3) after Sudden Cooling in Air at 750°C.

4 Discussion

Figure (2, 3, 4, and 5) show XRD analysis of the presence of main phases α - Cu3Zn, β CuZn, CuO, Cu_2O, Al_2Cu, Pb, and ZnO these Figure were carried out after oxidation; the presence of these phases play an important role in improving and developing the metallurgical, Corrosion resistance and oxidation behavior properties [24], [25]. On the other hand, Figure (6, 7, 8, 9) presented microstructure of all samples, there are (α, β) brass appear clearly in reference sample (B) Figure (6) with clear crystalline boundaries with dendrite grow this is expected (tree-like–structure) light Coarse plate grains of (α) and original grain of beta (β). Sample B1 (Cu-Zn-AL) structure was changed and became refined due to the addition of Al, which plays an essential parameter in increasing Zn concentration (Zn equivalent); increasing Zn % will refine the grains [26]. While Figure (8), which represented sample B2 (Cu-Zn-Al-Sn), the presence of Sn plays an essential role in changing the shape of microstructure; it prevents dendrite growth and increases refining; accordingly, the existence of an element (AI, Sn) will enhance solid solution strengthening, an increase in mechanical properties will be observed, for this reason, ductility of brass will decrease [27]. A change also occurs in the microstructure for specimen B3 (Cu-Zn-Al-Ge); the structure will change: equiaxed grain will appear due to the precipitation of free particles of Ge element on grain boundaries [28]. As a result of the significant change in the microstructure due to the addition of alloying elements, the hardness of Vickers is accompanied by a significant increase. Table (2) represents an improvement in Vicker values for all samples. Adding (AI, Sn, Ge) will increase Zn contrition (Zn equivalent), which solute in Cu and amount of substitution solid solution will increase, and grain refining will occur as discussed above. Figure (10) represents a cross–section SEM of base metal after cyclic oxidation at 600°C for 60 hrs. It can be found that the oxide layer exhibits defects such as voids, cracks, pores, and delamination. On the contrary, Figure (11,12) show cross–section SEM and EDS of alloy B3 oxidized at 600°C. There are no defects. A dense and coherent surface oxide layer lead to significant benefit protection, improving weight change at 750°C, reaching 98.9%, see Table (3).

Figure (13) represents the corrosive behavior of reference sample (B): dezincification; this behavior is expected because this alloy cannot build a protective layer in the salt solution. Zinc will preferentially leach out of alloy (more active than copper), leaving behind a copper-rich surface layer (porous and brittle). Zinc is selectively attacked if its concentration is more than 35% Zn [28]. However, when adding alloying elements, corrosive behavior changes significantly; Figure (14) shows the behavior of corrosion rate for all samples (B, B1, B2, B3); two notes can be made: first, adding alloying elements decrease corrosion behavior significantly, second: alloy (B3) show lower corrosion rate than B1, B2 after more than (170) days immersion in 3.5% NaCI this is due to the ability of this alloy to build protective layers of both (GeO_2, Al_2O_3) these phases appear in EDX and XRD . on the other hand, oxidation behavior of this sample (B3) see Table (3) and Figure (15 and 16), show better resistance at different temperature (500 to 750) °C comparing to other alloys (B, B1, B2) the addition of (Ge) improved oxidation resistance of this alloy many studies confirmed this fact that XRD and

EDs of this alloy confirmed the presence of GeO_2, Al_2O_3, these phases build protective layers, prevent any Cu+2, Zn+2 to diffuse through it [29].

Figure (18,19) represented the result of the thermal shock of all samples after cooling suddenly in the air after (60 hrs.) at 650 °C and 750 °C heating; base alloy showed severe oxidative, spalling, and black, while other samples showed better behavior, especially B3, which showed better behavior thermal Shock resistance comparing with others alloys (B1, B2) Figure (18,19). Thermal stress usually rises because there is a remarkable difference in thermal coefficient expansion between metal and its oxide and a sudden temperature change, resulting in the development of tension and compression stress leading to the cracking of the oxide layer oxide of Al_2O_3 [30]; GeO2 is more adherent to the surface, nonporous, also Ge element improve plasticity [31].

5 Conclusion

According to the results have been getting of the present work, the following points can be concluded:

- Alloying elements (Ge, Al, Sn) play an essential role in improving and enhancing properties of Munt Z metal (60%Cu – 40%Zn); adding (Ge) (0.3%) improves the oxidation resistance of alloy at different temperatures (500 to 750°C) better than (Al, Sn) as well as thermal shock, this improvement is attributed to the protective layer of GeO_2which is protective, non – porous, adhesive and more plasticity.
- Also, adding (Ge) improves corrosion resistance compared to the reference sample, which suffers from dezincification.
- Also, there is an enhancement in hardness value compared to the reference sample.

References

[1] S. Sattar, Y. Alaiwi, N. S. Radhi, and Z. Al-khafaji, "Numerical Simulation for Effect of Composite Coating (TiO2 + SiO2) Thickness on Steam Turbine Blades Thermal and Stress Distribution," *Academic Journal Of Manufacturing Engineering*, vol. 21, no. 4, 2023.

[2] N. S. RADHI, Z. AL-KHAFAJI, B. M. MAREAI, S. RADHI, and A. M. ALSAEGH, "Reducing Oil Pipes Corrosion By (Zn-Ni) Alloy Coating On Low Carbon Steel Substrate By Sustainable Process," *Journal of Engineering Science and Technology*, vol. 18, no. 3, pp. 1624–1638, 2023.

[3] S. Sattar *et al.*, "Corrosion reduction in steam turbine blades using nano-composite coating," *Journal of King Saud University-Science*, vol. 35, no. 8, p. 102861, 2023, doi: 10.1016/j.jksus.2023.102861.

[4] A. H. Jasim, N. S. Radhi, N. E. Kareem, Z. S. Al-Khafaji, and M. Falah, "Identification and investigation of corrosion behavior of electroless composite coating on steel substrate," *Open Engineering*, vol. 13, no. 1, p. 20220472, 2023.

[5] E. Mohammed and Z. Al-khafaji, "Effect of Surface Treatments by Ultrasonic on NiTi Biomaterials," *Academic Journal Of Manufacturing Engineering*, vol. 21, no. 3, pp. 1–6, 2023.

[6] N. S. Radhi, N. M. Sahi, and Z. Al-Khafaji, "Investigation Mechanical and Biological Properties of Hybrid PMMA Composite Materials as Prosthesis Complete Denture," *Egyptian Journal of Chemistry*, 2022, doi: 10.21608/EJCHEM.2022.110545.5034.

[7] Z. S. Al-khafaji, N. S. Radhi, and S. A. Mohson, "Preparation and modelling of composite materials (polyester-alumina) as implant in human body," *International Journal of Mechanical Engineering and Technology*, vol. 9, no. 4, 2018.

[8] N. M. Dawood, N. S. Radhi, and Z. S. Al-khafaji, "Investigation Corrosion and Wear Behavior of Nickel-Nano Silicon Carbide on Stainless Steel 316L," vol. 1002, pp. 33–43, 2020, doi: 10.4028/www.scientific.net/MSF.1002.33.

[9] N. S. Radhi and Z. Al-Khafaji, "Investigation biomedical corrosion of implant alloys in physiological environment," *International Journal of Mechanical and Production Engineering Research and Development*, vol. 8, no. 4, 2018, doi: 10.24247/ijmperdaug201827.

[10] H. A. Mohammed, G. Bhaskaran, N. H. Shuaib, and R. Saidur, "Heat transfer and fluid flow characteristics in microchannels heat exchanger using nanofluids: a review," *Renewable and Sustainable Energy Reviews*, vol. 15, no. 3, pp. 1502–1512, 2011.

[11] Z. Rajabi and H. Doostmohammadi, "Effect of addition of tin on the microstructure and machinability

of α-brass," *Materials Science and Technology*, vol. 34, no. 10, pp. 1218–1227, 2018.
[12] B. Al-Zubaidy, N. S. Radhi, and Z. S. Al-Khafaji, "Study the effect of thermal impact on the modelling of (titanium-titania) functionally graded materials by using finite element analysis," *International Journal of Mechanical Engineering and Technology*, no. 1, 2019.
[13] N. S. Radhi, A. H. Jasim, Z. S. Al-khafaji, and M. Falah, "Investigation of Hematite Nanoparticles According to Mechanical Characteristics of Aluminium Matrix Composite," *Nanosistemi, Nanomateriali, Nanotehnologii*, vol. 21, no. 4, pp. 769–778, 2023.
[14] N. D. Fahad, N. S. Radhi, Z. S. Al-Khafaji, and A. A. Diwan, "Surface modification of hybrid composite multilayers spin cold spraying for biomedical duplex stainless steel," *Heliyon*, 2023, doi: 10.1016/j.heliyon.2023.e14103.
[15] N. S. Aslan, A. K. Rajih, and A. H. Haleem, "Effect of Alloying Elements on the Erosion–Corrosion Behaviour of Cu-Based Alloys," in *IOP Conference Series: Materials Science and Engineering*, IOP Publishing, 2020, p. 12018.
[16] B. C. Syrett and A. Acharya, *Corrosion and degradation of implant materials*, vol. 684. ASTM International, 1979.
[17] Z. M. Abed Janabi, H. S. Jaber Alsalami, Z. S. Al-Khafaji, and S. A. Hussien, "Increasing of the corrosion resistance by preparing the trivalent nickel complex," *Egyptian Journal of Chemistry*, 2021, doi: 10.21608/EJCHEM.2021.100733.4683.
[18] H. J. Karim, K. F. Al-Sultani, and E. M. Saeed, "Improving Corrosion Resistance and Mechanical Properties of (60 % Cu / 40 % Zn) Alloy," *Test Engineering and managements*, vol. 83, no. 13024, pp. 13024–13034, 2020.
[19] J. R. Davis, *ASM specialty handbook: tool materials*. ASM international, 1995.
[20] U. Superseding, "USACE/NAVFAC/AFCESA/NASA UFGS 22 00 70 (February 2011)".
[21] A. HALLEM and I. N. KADHIM, "Improving Oxidation Behavior of (Alpha-Beta)(Cu-Zn40) Brass by Aluminum Addition," *International Journal of Mechanical and Production Engineering Research and Development (JMPERD)*, vol. 9, pp. 329–340, 2019.
[22] L. I. N. Gaoyong, Z. Yuxiong, Z. Juhua, Z. O. U. Yanming, L. I. U. Jian, and S. U. N. Liping, "Influence of rare earth elements on corrosion behavior of Al-brass in marine water," *Journal of Rare Earths*, vol. 29, no. 7, pp. 638–644, 2011.
[23] G. ASTM, "Standard reference test method for making potentiostatic and potentiodynamic anodic polarization measurements," *Annual book of ASTM Standards*, vol. 3, pp. 48–58, 2004.
[24] M. Jesiotr, W. Trzaskowski, D. Trochimiak, P. Nawrocki, K. Łukasik, and D. Myszka, "The Effect of Addition of Germanium to the Surface Phenomena in Silver Alloys," *Archives of Foundry Engineering*, vol. 18, no. 3, pp. 81–85, 2018.
[25] Z. Li and P. Tsakiropoulos, "The effect of Ge addition on the oxidation of Nb-24Ti-18Si silicide based alloys," *Materials*, vol. 12, no. 19, p. 3120, 2019.
[26] R. M. Hussein and O. I. Abd, "Influence of Al and Ti additions on microstructure and mechanical properties of leaded brass alloys," *Indian Journal of Materials Science*, vol. 2014, 2014.
[27] D. Suksongkarm, S. Rojananan, and S. Rojananan, "Microstructure and hardness of Cu-Zn-Si-Al-Sn brasses with antimony addition," in *Advanced Materials Research*, Trans Tech Publ, 2013, pp. 179–183.
[28] M. Hasnine, B. Tolla, and M. Karasawa, "Effect of Ge addition on wettability, copper dissolution, microstructural and mechanical behavior of SnCu–Ge solder alloy," *Journal of Materials Science: Materials in Electronics*, vol. 28, no. 21, pp. 16106–16119, 2017.
[29] M. K. Abbass, M. M. Radhi, and R. S. A. Adnan, "The effect of Germanium addition on mechanical properties& microstructure of Cu-Al-Ni shape memory alloy," *Materials Today: Proceedings*, vol. 4, no. 2, pp. 224–233, 2017.
[30] A. M. M. EI-Bahloul, M. Samuel, and M. K. I. AL-Mashhadani, "Improvement in the Wear Resistance of Brass Impeller of Slurry Pump used in Variation of Operating Speeds," *International Journal of Science and Engineering Applications*, vol. 4, no. 4, pp. 197–202, 2015, doi: 10.7753/ijsea0404.1007.
[31] K. M. Watling, A. Chandler-Temple, and K. Nogita, "XPS analysis of oxide films on lead-free solders with trace additions of germanium and gallium," in *Materials Science Forum*, Trans Tech Publ, 2016, pp. 63–67.